# Understanding $P_{cs}(4459)$ as a hadronic molecule in the $\Xi_b^- \to J/\psi\Lambda K^-$ decay

Jun-Xu Lu,[1,2] Ming-Zhu Liu,[1,2] Rui-Xiang Shi,[2] and Li-Sheng Geng[2,3,4,*]

[1]*School of Space and Environment, Beihang University, Beijing 102206, China*
[2]*School of Physics, Beihang University, Beijing 102206, China*
[3]*Beijing Key Laboratory of Advanced Nuclear Materials and Physics, Beihang University, Beijing 102206, China*
[4]*School of Physics and Microelectronics, Zhengzhou University, Zhengzhou, Henan 450001, China*

(Received 25 April 2021; accepted 28 June 2021; published 19 August 2021)

Recently, the LHCb Collaboration reported on the evidence for a hidden charm pentaquark state with strangeness, i.e., $P_{cs}(4459)$, in the $J/\psi\Lambda$ invariant mass distribution of the $\Xi_b^- \to J/\psi\Lambda K^-$ decay. In this work, assuming that $P_{cs}(4459)$ is a $\bar{D}^*\Xi_c$ molecular state, we study this decay via triangle diagrams $\Xi_b \to \bar{D}_s^{(*)}\Xi_c \to (\bar{D}^{(*)}\bar{K})\Xi_c \to P_{cs}\bar{K} \to (J/\psi\Lambda)\bar{K}$. Our study shows that the production yield of a spin $3/2$ $\bar{D}^*\Xi_c$ state is approximately one order of magnitude larger than that of a spin $1/2$ state due to the interference of $\bar{D}_s\Xi_c$ and $\bar{D}_s^*\Xi_c$ intermediate states. We obtain a model independent constraint on the product of couplings $g_{P_{cs}\bar{D}^*\Xi_c}$ and $g_{P_{cs}J/\psi\Lambda}$. With the predictions of two particular molecular models as inputs, we calculate the branching ratio of $\Xi_b^- \to (P_{cs} \to)J/\psi\Lambda K^-$ and compare it with the experimental measurement. We further predict the line shape of this decay that could be useful to future experimental studies.

DOI: 10.1103/PhysRevD.104.034022

## I. INTRODUCTION

In 2015, two pentaquark states $P_c(4380)$ and $P_c(4450)$ were observed in the $J/\psi p$ invariant mass distribution of the $\Lambda_b \to J/\psi pK^-$ decay by the LHCb Collaboration [1], which have long been anticipated theoretically [2–11]. Since then, a large amount of theoretical works have been performed to understand their nature. The most popular interpretations include $\bar{D}^{(*)}\Sigma_c^{(*)}$ molecular states [12–20], compact pentaquark states [21–23], and kinematical effects [24,25]. The experimental results were updated in 2019 with a data sample of almost ten times larger [26]. A new narrow state, $P_c(4312)$ was discovered. More interestingly, the original $P_c(4450)$ state splits into two states, $P_c(4440)$ and $P_c(4457)$. The masses and widths of these states are tabulated in Table I. After the 2019 update, the pentaquark states look more like $\bar{D}^{(*)}\Sigma_c^{(*)}$ molecules [27–40], but again nonmolecular interpretations are possible, such as compact pentaquark states [41–43] and even double triangle singularities [44].

Most recently, the LHCb Collaboration reported on the first evidence for a structure in the $J/\psi\Lambda$ invariant mass distribution of the $\Xi_b^- \to J/\psi\Lambda K^-$ decay [45], hinting at the existence of a pentaquark state with strangeness, i.e., $P_{cs}(4459)$. It should be noted that the existence of pentaquark states with strangeness was predicted together with their nonstrange counterparts in the molecular picture [2,3]. The $P_{cs}(4459)$ state is located close to the $\bar{D}^*\Xi_c$ threshold, leading naturally to a molecular interpretation [46–51]. One interesting point to be noted is that in addition to the four $P_c$s discovered experimentally, there may be three more candidates which strongly couple to $\bar{D}^*\Sigma_c^*$ with $J^P = \frac{1}{2}^-, \frac{3}{2}^-, \frac{5}{2}^-$, as dictated by the heavy quark spin symmetry [30,35,36,39]. As for pentaquark states with strangeness, one expects 10 of them [47,50,52,53].

In addition to the masses and widths of the pentaquark states, the LHCb Collaboration also reported the production yields of $P_c(4312)$, $P_c(4380)$, $P_c(4440)$, $P_c(4457)$, and $P_{cs}(4459)$, which are collected in Table I. One notes that the production yield for $P_c(4380)$ is one order of magnitude larger than that of $P_c(4312)$, which provides an explanation why $P_c(4312)$ was not observed in 2015. However, we note that the sum of the production yields of $P_c(4440)$ and $P_c(4457)$ is only half of that of $P_c(4450)$,

*Corresponding author.
lisheng.geng@buaa.edu.cn

TABLE I. Resonance parameters of the newly discovered pentaquark states and their production ratios, defined as $R = \frac{\mathcal{B}(\Lambda_b(\Xi_b)\to P_c(P_{cs})\bar{K})\mathcal{B}(P_c(P_{cs})\to J/\psi p(\Lambda))}{\mathcal{B}(\Lambda_b(\Xi_b)\to \bar{K}J/\psi p(\Lambda))}$.

| State | Mass (MeV) | Width (MeV) | $R(\%)$ |
|---|---|---|---|
| $P_c(4312)$ | $4311.9 \pm 0.7^{+6.8}_{-0.6}$ | $9.8 \pm 2.7^{+3.7}_{-4.5}$ | $0.30 \pm 0.07^{+0.34}_{-0.09}$ [26] |
| $P_c(4380)$ | $4380 \pm 8 \pm 29$ | $205 \pm 18 \pm 86$ | $8.4 \pm 0.7 \pm 4.2$ [1] |
| $P_c(4440)$ | $4440.3 \pm 1.3^{+4.1}_{-4.7}$ | $20.6 \pm 4.9^{+8.7}_{-10.1}$ | $1.11 \pm 0.33^{+0.22}_{-0.10}$ [26] $\quad 4.1 \pm 0.5 \pm 1.1$ [1] |
| $P_c(4457)$ | $4457.3 \pm 0.6^{+4.1}_{-1.7}$ | $6.4 \pm 2.0^{+5.7}_{-1.9}$ | $0.53 \pm 0.16^{+0.15}_{-0.13}$ [26] |
| $P_{cs}(4459)$ | $4458.8 \pm 2.9^{+4.7}_{-1.1}$ | $17.3 \pm 6.5^{+8.0}_{-5.7}$ | $2.7^{+1.9+0.7}_{-0.6-1.3}$ [45] |

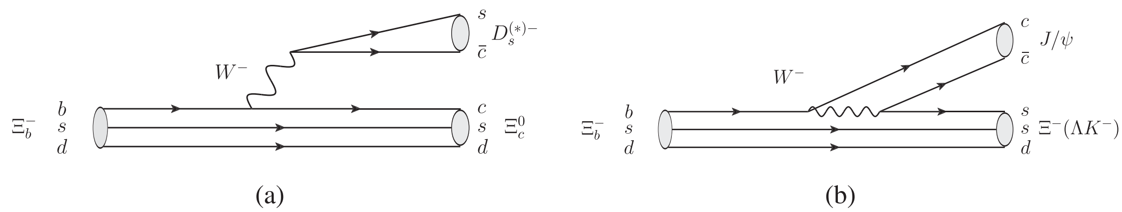


FIG. 1. External $W$-emission (a) and internal $W$-conversion (b) mechanism for the $\Xi_b$ decay.

which may indicate that something is missing, maybe a new resonance as suggested in several works [19,54–56]. Clearly, understanding the production yields, particularly the pattern shown in Table I, will greatly improve our understanding of the pentaquark states.[1]

In the present work, we study the branching ratio of $\Xi_b^- \to P_{cs}K^-$.[2] The present work differs from those of Refs. [64,65] in two ways. First, the weak production formalism is different from that of Ref. [64] (see also Ref. [66]), which allows for a prediction of the absolute branching ratio of the $\Xi_b^- \to P_{cs}K^- \to J/\psi\Lambda K^-$ decay within a molecular model. Compared to Ref. [65], we use different parametrizations of form factors and predict the line shape of the $\Xi_b^- \to P_{cs}K^- \to J/\psi\Lambda K^-$ decay. Taking two molecular models for the $P_{cs}(4459)$ state [47,51], we compare the so-obtained branching ratios with the experimental data. In the present work, we assume that the $P_{cs}$ state is dominantly a $\bar{D}^*\Xi_c$ bound state. Contributions from coupled channels with $\Xi_c'$ or $\Xi_c^*$ are suppressed in the weak decay of $\Xi_b$ due to their light axial-vector diquark. We also neglect the contributions from other channels such as $\bar{D}\Xi_c$ and $\bar{D}_s^{(*)}\Lambda_c$ because of the relatively larger gaps between the thresholds and the mass of $P_{cs}$. We note that the studies based on the unitary approach [47] and the one-boson-exchange model [51] have shown that the couplings of the $P_{cs}$ state to $\bar{D}\Xi_c$ and $\bar{D}_s^{(*)}\Lambda_c$ are much smaller than that to $\bar{D}^*\Xi_c$.

The present work is organized as follows. In Sec. II, we explain in detail the mechanism for the $P_{cs}(4459)$ production in the $\Xi_b^-$ decay, which involves a weak interaction part and a strong interaction part. In Sec. III, we present the numerical results and compare with the experimental data, followed by a short summary in Sec. IV.

## II. THEORETICAL FRAMEWORK

Assuming that $P_{cs}(4459)$ is a molecule mainly composed of $\bar{D}^*\Xi_c$, the $\Xi_b^- \to P_{cs}K^-$ decay can proceed as shown in diagram (a) of Fig. 1. The $\Xi_b$ state first decays into $\Xi_c$ by emitting a $W^-$ boson which is then converted into a pair of $\bar{c}s$, which after hadronization turns into a $D_s^{(*)}$. Next the $D_s^{(*)}$ meson emits a kaon and a $\bar{D}^*$. The final state interaction of $\bar{D}^*\Xi_c$ dynamically generates the $P_{cs}(4459)$ state which then decays into $J/\psi\Lambda$, as shown in Fig. 2.

In addition to the $W$-emission diagram discussed above, the $\Xi_b^-$ decay can also proceed via the internal $W$-exchange mechanism shown in Fig. 1(b). The $ssd$ cluster can either directly hadronize into a $\Xi^-$ or, by picking up a pair of $q\bar{q}$ from the vacuum, hadronizes into $\Lambda K^-$. The former is indeed a main decay channel of $\Xi_b^-$ [67], while the latter has been studied in Ref. [64].

### A. Branching ratio of $\Xi_b \to P_{cs}K^-$

In the following, we describe how to calculate the diagrams of Fig. 2. The effective Lagrangian responsible for the $\Xi_b \to \Xi_c\bar{D}_s^{(*)}$ decay reads

[1]We note that recently the electromagnetic properties of the pentaquark states have been studied [57–62], which, if measured, could also help improve our understanding of these states.

[2]In Ref. [63], a similar mechanism has been applied to study the $D_s^+ \to \pi^+\pi^0\eta$ decay and it is shown that both the branching ratio and the $\pi^{+(0)}\eta$ line shape are well described. In particular, the large branching ratio of $D_s^+ \to a_0^+\pi^0(a_0^0\pi^+)$ is naturally explained, while for a pure $W$-annihilation process one would expect a much smaller value.

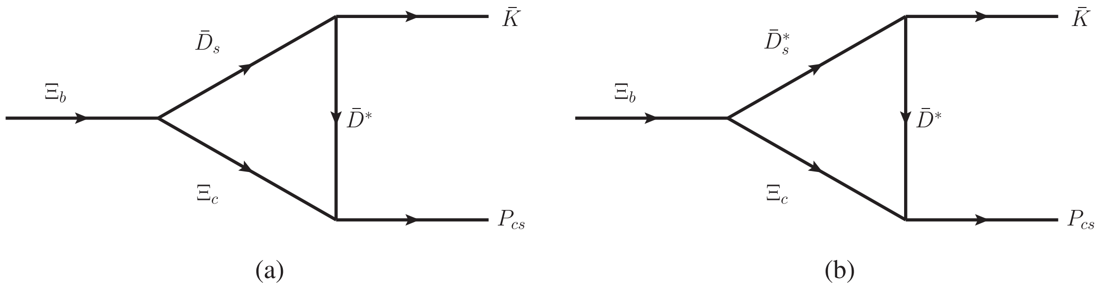


FIG. 2. Triangle diagrams for the $\Xi_b^- \to P_{cs}K^-$ decay.

$$\mathcal{L}_{\Xi_b\Xi_c D_s} = i\bar{\Xi}_c(A+B\gamma_5)\Xi_b D_s,$$
$$\mathcal{L}_{\Xi_b\Xi_c D_s^*} = \bar{\Xi}_c\left(A_1\gamma_\mu\gamma_5 + A_2\frac{p_{2\mu}}{m}\gamma_5 + B_1\gamma_\mu + B_2\frac{p_{2\mu}}{m}\right)\Xi_b D_s^{*\mu}. \quad (1)$$

The $A_1$, $A_2$, $B_1$, $B_2$, $A$, and $B$ can be expressed with the six form factors describing the $\Xi_b \to \Xi_c$ transition [68] as[3]

$$A = \lambda f_{D_s}\left[(m-m_2)f_1^V + \frac{m_1^2}{m}f_3^V\right],$$
$$B = \lambda f_{D_s}\left[(m+m_2)f_1^A - \frac{m_1^2}{m}f_3^A\right],$$
$$A_1 = -\lambda f_{D_s^*}m_1\left[f_1^A - f_2^A\frac{m-m_2}{m}\right],$$
$$B_1 = \lambda f_{D_s^*}m_1\left[f_1^V + f_2^V\frac{m+m_2}{m}\right],$$
$$A_2 = 2\lambda f_{D_s^*}m_1 f_2^A, \qquad B_2 = -2\lambda f_{D_s^*}m_1 f_2^V, \quad (2)$$

where $\lambda = \frac{G_F}{\sqrt{2}}V_{cb}V_{cs}a_1$ with $a_1 = 1.07$ [70]. The decay constants $f_{D_s^{(*)}}$ for $\bar{D}_s$ and $\bar{D}_s^*$ are set to be 0.247 GeV and $m, m_1, m_2$ refer to the masses of $\Xi_b$, $\bar{D}_s^{(*)}$, and $\Xi_c$ respectively.

Following the double-pole parametrization proposed in Ref. [71], one can rewrite the form factors as

$$f_i^{V/A}(q^2) = F_i^{V/A}(0)\frac{\Lambda_1^2}{q^2-\Lambda_1^2}\frac{\Lambda_2^2}{q^2-\Lambda_2^2}. \quad (3)$$

Fitting to the results of the relativistic quark-diquark model [69], we can obtain the values of $F(0)$, $\Lambda_1$, and $\Lambda_2$, which are tabulated in Table II.

The effective Lagrangians for the $P_{cs} \to \bar{D}^*\Xi_c$ and $\bar{D}_s^{(*)} \to \bar{D}^*\bar{K}$ read

$$\mathcal{L}_{P_{cs1}\Xi_c\bar{D}^*} = g_{P_{cs1}\Xi_c\bar{D}^*}\bar{\Xi}_c\gamma_5\left(g_{\mu\nu} - \frac{p_\mu p_\nu}{m_{P_{cs}}^2}\right)\gamma^\nu P_{cs1}D^{*\mu},$$
$$\mathcal{L}_{P_{cs2}\Xi_c\bar{D}^*} = g_{P_{cs2}\Xi_c\bar{D}^*}\bar{\Xi}_c P_{cs2\mu}D^{*\mu},$$
$$\mathcal{L}_{P_{cs1}J/\psi\Lambda} = g_{P_{cs1}J/\psi\Lambda}\bar{\Lambda}\gamma_5\left(g_{\mu\nu} - \frac{p_\mu p_\nu}{m_{P_{cs}}^2}\right)\gamma^\nu P_{cs1}J/\psi^\mu,$$
$$\mathcal{L}_{P_{cs2}J/\psi\Lambda} = g_{P_{cs2}J/\psi\Lambda}\bar{\Lambda}P_{cs2\mu}J/\psi^\mu,$$
$$\mathcal{L}_{KD_sD^*} = ig_{KD_sD^*}D^{*\mu}[\bar{D}_s\partial_\mu K - (\partial_\mu\bar{D}_s)K] + \mathrm{H.c.},$$
$$\mathcal{L}_{KD_s^*D^*} = -g_{KD_s^*D^*}\epsilon^{\mu\nu\alpha\beta}[\partial_\mu\bar{D}_\nu^*\partial_\alpha D_{s\beta}^*\bar{K} + \partial_\mu D_\nu^*\partial_\alpha\bar{D}_{s\beta}^*K] + \mathrm{H.c.}, \quad (4)$$

where $P_{cs1}$ and $P_{cs2}$ denote the $P_{cs}(4459)$ state with $J^P = \frac{1}{2}^-$ and $\frac{3}{2}^-$, respectively. The $g_{KD_sD^*}$ and $g_{KD_s^*D^*}$ are the kaon meson couplings to $D_sD^*$ and $D_s^*D^*$, respectively.

TABLE II. Parameters $F(0)$, $\Lambda_1$, $\Lambda_2$ in the form factors of the $\Xi_b \to \Xi_c$ transition form factors.

| | $F_1^V$ | $F_2^V$ | $F_3^V$ | $F_1^A$ | $F_2^A$ | $F_3^A$ |
|---|---|---|---|---|---|---|
| $F(0)$ | 0.467 | 0.145 | 0.086 | 0.447 | −0.035 | −0.278 |
| $\Lambda_1$( GeV) | 5.10 | 4.89 | 6.14 | 4.69 | 4.97 | 4.58 |
| $\Lambda_2$( GeV) | 9.03 | 5.46 | 6.28 | 12.20 | 5.05 | 7.08 |

[3]Here we adopt the convention for the form factors of Ref. [69] in which there exists an extra minus in front of $f_2^A$ and $f_2^V$.

We take $g_{KD_sD^*} = 5.0$ and $g_{KD_s^*D^*} = 7.0\ \mathrm{GeV}^{-1}$ in the present work, which are extracted from Ref. [72]. The $g_{P_{cs1}\Xi_c\bar{D}^*}$, $g_{P_{cs2}\Xi_c\bar{D}^*}$, $g_{P_{cs1}J/\psi\Lambda}$, and $g_{P_{cs2}J/\psi\Lambda}$ are the couplings between $P_{cs}$ and its components, whose values are not known *a priori*, but they can be computed with the compositeness conditions [73–75] or in molecular models, e.g., Ref. [47,51], or in lattice QCD.

With the effective Lagrangians above, the decay amplitudes for $\Xi_b(p) \to \bar{D}_s^{(*)}(p_1)\Xi_c(p_2)[\bar{D}^*(q)] \to \bar{K}(p_3)P_{cs1}(p_4)$ read

$$
\begin{aligned}
\mathcal{M}_{P_{cs1}} &= \mathcal{M}_{\bar{D}_s}^{P_{cs1}} + \mathcal{M}_{\bar{D}_s^*}^{P_{cs1}}, \\
\mathcal{M}_{\bar{D}_s}^{P_{cs1}} &= i^3 \int \frac{d^4 q}{(2\pi)^4} \left[ g_{P_{cs1}\Xi_c\bar{D}^*} \bar{u}(p_4)\gamma^\nu\gamma_5 \left( g_{\mu\nu} - \frac{p_{4\mu}p_{4\nu}}{m_4^2} \right) \right] (\not{p}_2 + m_2) \\
&\quad \times [i(A + B\gamma_5)u(p)][-g_{KD^*D_s}(p_1 + p_3)_\alpha] \left( -g^{\mu\alpha} + \frac{q^\mu q^\alpha}{m_E^2} \right) \\
&\quad \times \frac{1}{p_1^2 - m_1^2} \frac{1}{p_2^2 - m_2^2} \frac{1}{q^2 - m_E^2} \mathcal{F}(q^2, m_E^2), \\
\mathcal{M}_{\bar{D}_s^*}^{P_{cs1}} &= i^3 \int \frac{d^4 q}{(2\pi)^4} \left[ g_{P_{cs1}\Xi_c\bar{D}^*} \bar{u}(p_4)\gamma^\nu\gamma_5 \left( g_{\mu\nu} - \frac{p_{4\mu}p_{4\nu}}{m_4^2} \right) \right] (\not{p}_2 + m_2) \\
&\quad \times \left[ \left( A_1\gamma_\alpha\gamma_5 + A_2 \frac{p_{2\alpha}}{m}\gamma_5 + B_1\gamma_\alpha + B_2 \frac{p_{2\alpha}}{m} \right) u(p) \right] \\
&\quad \times [-g_{KD^*D_s^*}\varepsilon_{\rho\lambda\eta\tau} q^\rho p_1^\eta] \left( -g^{\mu\lambda} + \frac{q^\mu q^\lambda}{m_E^2} \right) \left( -g^{\alpha\tau} + \frac{p_1^\alpha p_1^\tau}{m_1^2} \right) \\
&\quad \times \frac{1}{p_1^2 - m_1^2} \frac{1}{p_2^2 - m_2^2} \frac{1}{q^2 - m_E^2} \mathcal{F}(q^2, m_E^2).
\end{aligned} \tag{5}
$$

The decay amplitudes of $\Xi_b(p) \to \bar{D}_s^{(*)}(p_1)\Xi_c(p_2)[\bar{D}^*(q)] \to \bar{K}(p_3)P_{cs2}(p_4)$ read

$$
\begin{aligned}
\mathcal{M}_{P_{cs2}} &= \mathcal{M}_{\bar{D}_s}^{P_{cs2}} + \mathcal{M}_{\bar{D}_s^*}^{P_{cs2}}, \\
\mathcal{M}_{\bar{D}_s}^{P_{cs2}} &= i^3 \int \frac{d^4 q}{(2\pi)^4} [-i g_{P_{cs2}\Xi_c\bar{D}^*} \bar{u}_\mu(p_4)] (\not{p}_2 + m_2) [i(A + B\gamma_5) \\
&\quad \times u(p)][-g_{KD^*D_s}(p_1 + p_3)_\nu] \left( -g^{\mu\nu} + \frac{q^\mu q^\nu}{m_E^2} \right) \frac{1}{p_1^2 - m_1^2} \frac{1}{p_2^2 - m_2^2} \frac{1}{q^2 - m_E^2} \mathcal{F}(q^2, m_E^2), \\
\mathcal{M}_{\bar{D}_s^*}^{P_{cs2}} &= i^3 \int \frac{d^4 q}{(2\pi)^4} [-i g_{P_{cs2}\Xi_c\bar{D}^*} \bar{u}_\sigma(p_4)] (\not{p}_2 + m_2) \\
&\quad \times \left[ \left( A_1\gamma_\rho\gamma_5 + A_2 \frac{p_{2\rho}}{m}\gamma_5 + B_1\gamma_\rho + B_2 \frac{p_{2\rho}}{m} \right) u(p) \right] \\
&\quad \times [-g_{KD^*D_s^*}\varepsilon_{\mu\nu\alpha\beta} q^\mu p_1^\alpha] \left( -g^{\sigma\nu} + \frac{q^\sigma q^\nu}{m_E^2} \right) \left( -g^{\rho\beta} + \frac{p_1^\rho p_1^\beta}{m_1^2} \right) \\
&\quad \times \frac{1}{p_1^2 - m_1^2} \frac{1}{p_2^2 - m_2^2} \frac{1}{q^2 - m_E^2} \mathcal{F}(q^2, m_E^2),
\end{aligned} \tag{6}
$$

with $m_E$ the mass of the exchanged $\bar{D}^*$ mesons.

We follow Ref. [37] and introduce a monopole form factor to depict the off-shell effect of the exchanged $\bar{D}^*$ mesons,

$$
\mathcal{F}(q^2, m^2) = \frac{m^2 - \Lambda^2}{q^2 - \Lambda^2}, \tag{7}
$$

where $\Lambda = m + \alpha\Lambda_{\mathrm{QCD}}$ with $\Lambda_{\mathrm{QCD}} = 220$ MeV, and $\alpha$ is a model parameter. In this way, the triangle diagrams are free of any ultraviolet divergence. Collecting all the pieces together, the decay width for $\Xi_b \to P_{cs}\bar{K}$ could be expressed as

$$
\Gamma = \frac{1}{2J + 1} \frac{1}{8\pi} \frac{1}{m_{\Xi_b}^2} |\vec{p}| \sum |\mathcal{M}_{P_{cs1}/P_{cs2}}|^2, \tag{8}
$$

where $|\vec{p}|$ denotes the momentum of $\bar{K}$ or $P_{cs}$ in the rest frame of $\Xi_b$.

### B. $J/\psi\Lambda$ invariant mass distribution of the $\Xi_b^- \to K^- P_{cs} \to K^- J/\psi\Lambda$

With the weak decay vertices described in Eqs. (1) and (2), we can further work out the invariant mass distribution of the $\Xi_b^- \to J/\psi\Lambda K^-$ decay. Parametrizing the intermediate $P_{cs}(4459)$ state with a Breit-Wigner resonance, the amplitudes of Fig. 3 read

$$\begin{aligned}
\mathcal{A} &= \mathcal{A}_{\bar{D}_s} + \mathcal{A}_{\bar{D}_s^*},\\
\mathcal{A}_{\bar{D}_s} &= i\int \frac{d^4q}{(2\pi)^4}\bar{u}(p_5)\epsilon^\mu(p_4)\mathcal{A}_{\mu\alpha P_{cs1}/P_{cs2}}\cdot(\not{p}_2+m_2)\cdot\mathcal{A}_{\Xi_b\Xi_c\bar{D}_s}u(P)\\
&\quad\times\frac{\mathcal{A}^\alpha_{KD_sD^*}\cdot(-g_{\mu\alpha}+\frac{q^\mu q^\alpha}{m_E^2})}{(p_2^2-m_2^2)(p_1^2-m_1^2)(q^2-m_E^2)}\mathcal{F}(q^2,m_E^2),\\
\mathcal{A}_{\bar{D}_s^*} &= i\int \frac{d^4q}{(2\pi)^4}\bar{u}(p_5)\epsilon^\mu(p_4)\mathcal{A}_{\mu\alpha P_{cs1}/P_{cs2}}\cdot(\not{p}_2+m_2)\cdot\mathcal{A}^\beta_{\Xi_b\Xi_c\bar{D}_s^*}u(P)\\
&\quad\times\frac{\mathcal{A}^{\nu\beta}_{KD_s^*D^*}\cdot(-g_{\mu\nu}+\frac{q^\mu q^\nu}{m_E^2})(-g_{\alpha\beta}+\frac{q^\alpha q^\beta}{m_1^2})}{(p_2^2-m_2^2)(p_1^2-m_1^2)(q^2-m_E^2)}\mathcal{F}(q^2,m_E^2),
\end{aligned}\tag{9}$$

where $(p_4+p_5)^2 = p_{45}^2 = M_{45}^2$ denotes the invariant mass of the $J/\psi\Lambda$ final state and

$$\begin{aligned}
\mathcal{A}_{\Xi_b\Xi_c\bar{D}_s} &= i(A+B\gamma_5),\\
\mathcal{A}^\rho_{\Xi_b\Xi_c\bar{D}_s^*} &= A_1\gamma_\rho\gamma_5 + A_2\frac{p_{2\rho}}{m}\gamma_5 + B_1\gamma_\rho + B_2\frac{p_{2\rho}}{m},\\
\mathcal{A}^\alpha_{KD_sD^*} &= -g_{KD_sD^*}(p_1^\alpha+p_3^\alpha),\\
\mathcal{A}^{\nu\beta}_{KD_s^*D^*} &= -g_{KD_s^*D^*}\epsilon_{\mu\nu\alpha\beta}(q^\mu p_1^\alpha),\\
\mathcal{A}^{\mu a}_{P_{cs1}} &= \frac{g_{P_{cs1}\Xi_c\bar{D}^*}g_{P_{cs1}J/\psi\Lambda}}{p_{45}^2-m_{P_{cs}^2}+i\Gamma_{P_{cs}}m_{Pcs}}\gamma_5\left(g^{\mu\nu}-\frac{p_{45}^\mu p_{45}^\nu}{m_{P_{cs}}^2}\right)\gamma_\nu\cdot(\not{p}_{45}+m_{P_{cs}})\cdot\gamma_5\left(g_{ab}-\frac{p_{45}^a p_{45}^b}{m_{P_{cs}}^2}\right)\gamma_b,\\
\mathcal{A}^{\mu\nu}_{P_{cs2}} &= \frac{g_{P_{cs2}\Xi_c\bar{D}^*}g_{P_{cs2}J/\psi\Lambda}}{p_{45}^2-m_{P_{cs}^2}+i\Gamma_{P_{cs}}m_{P_{cs}}}(\not{p}_{45}+m_{P_{cs}})\cdot\left(-g^{\mu\nu}+\frac{\gamma^\mu\gamma^\nu}{d-1}+\frac{\gamma^\mu p_{45}^\nu-\gamma^\nu p_{45}^\mu}{(d-1)m_{P_{cs}}}+\frac{d-2}{(d-1)m_{P_{cs}}^2}p_{45}^\mu p_{45}^\nu\right).
\end{aligned}$$

The partial decay rate for $\Xi_b \to J/\psi\Lambda\bar{K}$ as a function of the invariant mass $M_{J/\psi\Lambda}$ then reads

$$\frac{d\Gamma}{dM_{J/\psi\Lambda}} = \frac{1}{2J+1}\frac{1}{64\pi^3}\frac{1}{m_{\Xi_b}^2}|p_3^*||p_4|\sum|\mathcal{A}|^2,\tag{10}$$

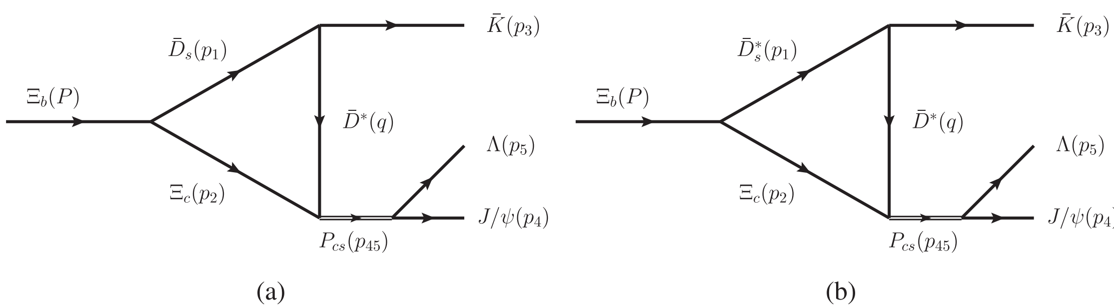


FIG. 3. Feynman diagrams for the $\Xi_b^- \to (P_{cs} \to)J/\psi\Lambda K^-$ decay.

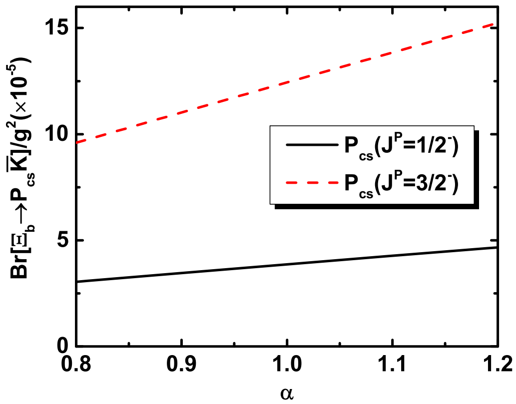


FIG. 4. Dependence of the branching ratios $\mathrm{Br}[\Xi_b \to P_{cs}\bar{K}]$ on $\alpha$.

with

$$p_3^* = \frac{\sqrt{(m_{\Xi_b}^2 - (m_K - M_{J/\psi\Lambda})^2)(m_{\Xi_b}^2 - (m_K + M_{J/\psi\Lambda})^2)}}{2m_{\Xi_b}},$$
$$p_4 = \frac{\sqrt{(M_{J/\psi\Lambda}^2 - (m_{J/\psi} - m_\Lambda)^2)(M_{J/\psi\Lambda}^2 - (m_{J/\psi} + m_\Lambda)^2)}}{2M_{J/\psi\Lambda}}. \tag{11}$$

## III. RESULTS AND DISCUSSIONS

In this section, we explore the decay mechanism proposed in this work. We divide our discussions into two categories, those which only depend on the decay mechanism explored and those which depend on a particular molecular model.

In our framework, the parameter $\alpha$ is not known, though its value is often assumed to be about 1 [76–79]. Therefore, we first study how the calculated branching ratios depend on the value of $\alpha$. Varying $\alpha$ from 0.8 to 1.2, we plot the values of $\mathrm{Br}[\Xi_b \to P_{cs1}(P_{cs2})\bar{K}]/g^2_{P_{cs1/2}\Xi_c\bar{D}^*}$ in Fig. 4. One can see that the branching ratios for $P_{cs1}$ and $P_{cs2}$ are moderately sensitive to the value of $\alpha$ in the range studied. As a consequence, in the following, we will take $\alpha = 1.0 \pm 0.1$ to take into account the uncertainties from $\alpha$.

### A. Model independent predictions

To compute the absolute branching ratio $\mathrm{Br}[\Xi_b \to P_{cs}\bar{K}]$, we need to know the coupling constants $g_{P_{cs1}\Xi_c\bar{D}^*}$ and $g_{P_{cs2}\Xi_c\bar{D}^*}$. They can be determined model independently with the compositeness conditions [73–75], as was done in, e.g., Ref. [32] for the pentaquark states. With the experimental mass of $P_{cs}$, the couplings read $g_{P_{cs1}\Xi_c\bar{D}^*} = 1.59$ and $g_{P_{cs2}\Xi_c\bar{D}^*} = 2.76$, corresponding to a cutoff $\Lambda = 1.0$ GeV (more details can be found in the Appendix). With these couplings, we find, surprisingly, that the branching ratio for the $P_{cs}$ state with $J^P = 3/2^-$ is approximately one order of magnitude larger than that for the $P_{cs}$ state with $J^P = 1/2^-$, which are

$$\mathrm{Br}[\Xi_b \to P_{cs1}\bar{K}] = (9.84 \pm 1.04) \times 10^{-5},$$
$$\mathrm{Br}[\Xi_b \to P_{cs2}\bar{K}] = (9.48 \pm 1.08) \times 10^{-4}. \tag{12}$$

In addition, using the experimental branching ratio $\mathrm{Br}[\Xi_b \to J/\psi\Lambda\bar{K}] = (2.31 \pm 1.37) \times 10^{-4}$ (see the Appendix on how to derive this), the mass, width, and branching ratio $R$ of the $P_{cs}$ state given in Table I as inputs, we can provide a model independent constraint on the product of the two couplings in Eq. (4), $g_{P_{cs}\bar{D}^*\Xi_c}$ and $g_{P_{cs}J/\psi\Lambda}$, within the decay mechanism studied in the present work. The experimental branching ratio given in Table I is $R = 2.7^{+2.0}_{-1.4}\%$. Using the formalism detailed in Sec. II B, we obtain

$$g_{P_{cs}\Xi_c\bar{D}^*}\, g_{P_{cs}J/\psi\Lambda} = \begin{cases} 0.18^{+0.10}_{-0.08} & \text{for } J^P = \frac{1}{2}^- \\ 0.17^{+0.10}_{-0.08} & \text{for } J^P = \frac{3}{2}^- \end{cases}. \tag{13}$$

The above product can be used to constrain molecular models.

### B. Comparison with models

In order to produce the branching ratio $R$ defined in the introduction, in addition to the information derived above, we need to know the partial decay width of $P_{cs}$ into $J/\psi\Lambda$. For this, we turn to specific molecular models. In the following, we study the unitary approach of Ref. [47] and the one-boson-exchange (OBE) model of Ref. [51], calculate the branching ratio $R$, and compare with the LHCb measurement.

First, we focus on Ref. [47]. Note that the difference between the definition of their couplings and ours (see the Appendix for details) and with the branching ratios $\mathrm{Br}[P_{cs} \to J/\psi\Lambda] = 3.31\%$ for $P_{cs1}$ and 14.68% for $P_{cs2}$ from Ref. [47], we obtain the couplings as $g_{P_{cs1}J/\psi\Lambda} = 0.07$ and $g_{P_{cs2}J/\psi\Lambda} = 0.27$. The branching ratios $R$ for the spin-parity assignment $1/2^-$ and $3/2^-$ are found to be

$$R_{P_{cs1}} = \frac{\mathrm{Br}[\Xi_b \to P_{cs1}\bar{K}]\mathrm{Br}[P_{cs1} \to J/\psi\Lambda]}{\mathrm{Br}[\Xi_b \to J/\psi\Lambda\bar{K}]} = 1.4 \pm 0.8\%,$$
$$R_{P_{cs2}} = \frac{\mathrm{Br}[\Xi_b \to P_{cs2}\bar{K}]\mathrm{Br}[P_{cs2} \to J/\psi\Lambda]}{\mathrm{Br}[\Xi_b \to J/\psi\Lambda\bar{K}]} = 60.3 \pm 36.4\%. \tag{14}$$

In the OBE model of Ref. [51], the $P_{cs}(4459)$ state is interpreted as a $J^P = 3/2^-$ molecular state and the partial decay width of $P_{cs} \to J/\psi\Lambda$ is estimated to be 0.06–0.2 MeV. The main decay mode is found to be $P_{cs} \to K^*\Xi(\omega\Lambda)$, which accounts for 80% of the total decay width. These numbers lead to an even smaller branching ratio $\mathrm{Br}[P_{cs} \to J/\psi\Lambda] = 0.6\% - 0.8\%$ corresponding to the total decay width ranging from 10 to 25 MeV. For the coupling between the $P_{cs}$ state with $J^P = 3/2^-$ and its components, we adopt the value

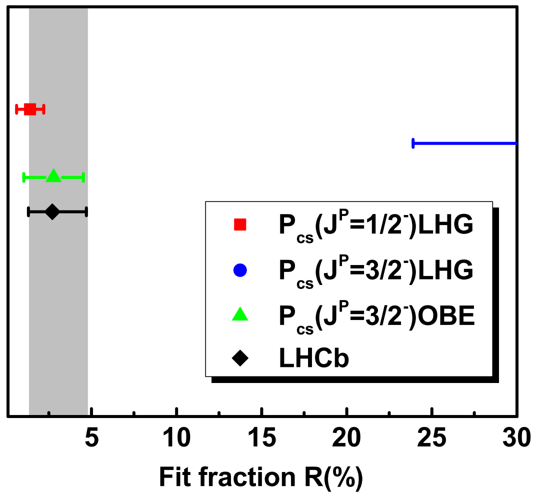


FIG. 5. Branching ratios $R$ for $P_{cs1}(J^P = 1/2^-)$ and $P_{cs2}(J^P = 3/2^-)$. The red square and blue circle denote our results given in Eq. (14), while the black diamond denotes the LHCb measurement [45]. The results with the partial decay width obtained from the OBE model of Ref. [51] (green triangle) is also shown for comparison.

$g_{P_{cs2}\Xi_c\bar{D}^*} = 2.76$ obtained from the compositeness condition. Using 0.7% as the central value for $\mathrm{Br}[P_{cs} \to J/\psi\Lambda]$ and 0.1% as its error, we obtain

$$R_{P_{cs2}} = \frac{\mathrm{Br}[\Xi_b \to P_{cs2}\bar{K}]\mathrm{Br}[P_{cs2} \to J/\psi\Lambda]}{\mathrm{Br}[\Xi_b \to J/\psi\Lambda\bar{K}]} = 2.87 \pm 1.75\%. \tag{15}$$

All these numbers are compared with the LHCb measurement in Fig. 5. It is clear that the result of the OBE model seems to agree with the experimental measurement, as well as the $J^P = 1/2^-$ case of the unitary approach.[4] The predicted branching ratio for $J^P = 3/2^-$ in the unitary approach is however much larger than the experimental number. Alternatively, one can also compare the product of $g_{P_{cs}\Xi_c\bar{D}^*}$ and $g_{P_{cs}J/\psi\Lambda}$ obtained from the two models with the values predicted model independently in Eq. (13). With the couplings of the $P_{cs}$ state to the components obtained in the Appendix, the products in the unitary approach read

$$\begin{aligned} g_{P_{cs1}\Xi_c\bar{D}^*}g_{P_{cs1}J/\psi\Lambda} &= 0.111 \quad \text{for } J^P = \frac{1}{2}^-, \\ g_{P_{cs2}\Xi_c\bar{D}^*}g_{P_{cs2}J/\psi\Lambda} &= 0.745 \quad \text{for } J^P = \frac{3}{2}^-, \end{aligned} \tag{16}$$

while in the OBE model, one has

$$g_{P_{cs2}\Xi_c\bar{D}^*}g_{P_{cs2}J/\psi\Lambda} = 0.180 \quad \text{for } J^P = \frac{3}{2}^-, \tag{17}$$

where we have adopted $g_{P_{cs2}\Xi_c\bar{D}^*} = 2.76$ determined via the compositeness condition as was done in Eqs. (14) and (15) because it was not given in Ref. [51]. We find that both the two products for the $J^P = 1/2^-$ and $3/2^-$ $P_{cs}$ states obtained from the unitary approach [47] are not quite consistent with the predicted values. The product for the $J^P = 1/2^-$ case locates close to the lower limit and, correspondingly, the central value of the predicted branching ratio is also close to the lower edge of the experimental measurement, as is shown in Fig. 5. For the $J^P = 3/2^-$ case, the product is over four times the size of the model independent estimate.[5] Thus, a much larger branching ratio is naturally foreseeable. On the other hand, the product from the OBE model is in good agreement with the model independent estimate. We note that the OBE model [51] differs from the unitary approach [47] in that they considered different coupled channels. In the OBE model, the lighter channels such as $\omega\Lambda$ and $K^*\Xi$ account for about 80% of the total decay width of $P_{cs}$, while in the unitary approach, the $J/\psi\Lambda$ and $\bar{D}_s^*\Lambda_c$ modes dominate the decay width.

Finally, in Fig. 6, we show the $J/\psi\Lambda$ invariant mass distribution of the $\Xi_b^- \to J/\psi\Lambda K^-$ decay with all the relevant couplings provided by the unitary approach of Ref. [47] (see the Appendix for more details). They might be useful for future experimental searches.

## IV. SUMMARY

In this work, we studied the decay of $\Xi_b^- \to P_{cs}K^- \to J/\psi\Lambda K^-$ via a triangle mechanism. The decay consists of three steps. First, $\Xi_b^-$ decays weakly into $\bar{D}_s^{(*)}$ and $\Xi_c$ via the external $W$-emission diagram. Using the relevant form factors determined in the relativistic quark-diquark model, this weak interaction part can be computed without any free parameters. Followed by the creation of $\bar{D}_s^{(*)}$ and $\Xi_c$ in the first step, the $\bar{D}_s^{(*)}$ state then emits a kaon and a $\bar{D}^*$. The $\bar{D}^*$ and $\Xi_c$ interact with each other to dynamically generate the $P_{cs}(4459)$ state, which then decays into $J/\psi\Lambda$. From such a decay mechanism, we derived a constraint on the product of couplings of the $P_{cs}(4459)$ state to the $\bar{D}^*\Xi_c$ and $J/\psi\Lambda$ channels. Determining the coupling between $P_{cs}$ and the $\bar{D}^*\Xi_c$ channel using the compositeness condition, we predicted the branching ratio $\mathrm{Br}[\Xi_b^- \to P_{cs}K^-]$. These can be useful to understanding the nature of $P_{cs}(4459)$ as a molecular state.

Using the predicted couplings by the unitary approach [47] and the one-boson-exchange model of Ref. [51], we calculated the branching ratios $\mathrm{Br}[\Xi_b^- \to (P_{cs} \to) J/\psi\Lambda K^-]$.

[4]We note that in the QCD sum rule approach of Ref. [80], it was shown that the assignment of the $P_{cs}(4459)$ state as a diquark-diquark-antiquark structure with $J^P = 1/2^-$ is possible by studying its strong decay to $J/\psi\Lambda$.

[5]Note that the decay width of $P_{cs}$ obtained from the two models are not exactly the central value of the experimental data with which the model independent products are derived.

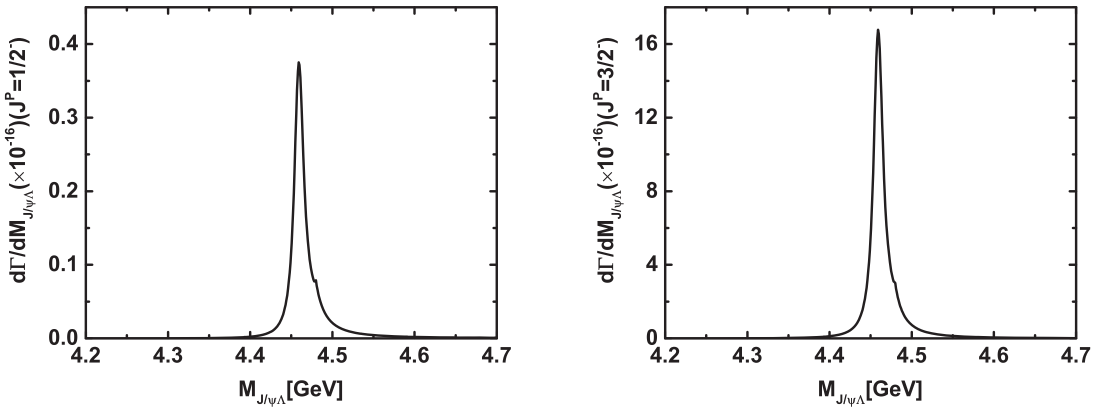


FIG. 6. Invariant mass distribution of $\Xi_b^- \to P_{cs}K^- \to J/\psi\Lambda K^-$ for $P_{cs}$ with $J^P = 1/2^-$ (left) and $J^P = 3/2^-$ (right).

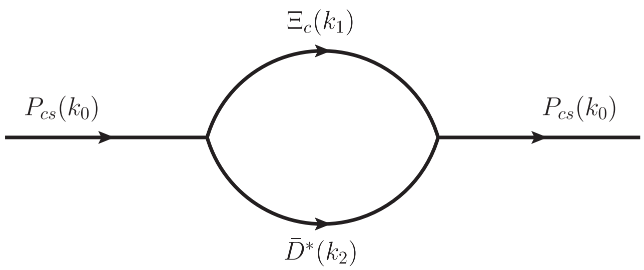


FIG. 7. Mass operators of the $P_c$.

We found that in the unitary approach, the $J^P = 1/2^-$ assignment is preferred, while the $J^P = 3/2^-$ assignment gives a branching ratio much larger than the experimental measurement. On the other hand, the $3/2$ assignment in the one-boson-exchange model of Ref. [51] yields a branching ratio in agreement with the LHCb data. This can be traced back to the drastically different partial decay width of $P_{cs} \to J/\psi\Lambda$.

In principle, the present formalism can also be utilized to study the $\Lambda_b \to J/\psi pK^-$ decay, where the four pentaquark states, $P_c(4312)$, $P_c(4380)$, $P_c(4440)$, and $P_c(4457)$, were discovered. This has been explored in Ref. [37], which, however, suffers from the fact that the weak decay $\Lambda_b \to \bar{D}_s^{(*)}\Sigma_c$ is suppressed because the $ud$ quark pair in $\Lambda_b$ has spin 0, but that in $\Sigma_c$ has spin 1. As a result, the relevant transition form factors are not known and therefore one could not arrive at a quantitative determination of the branching ratios. In addition, compared to the present case, the suppression of the $\Lambda_b \to \bar{D}_s^{(*)}\Sigma_c$ transition indicates that other mechanisms may play a role in addition to the external $W$-emission studied in the present work, which complicates the study a lot.

## ACKNOWLEDGMENTS

We thank Qi Wu, Dian-Yong Chen, and Li-Ming Zhang for useful communications. This work is partly supported by the National Natural Science Foundation of China under Grants No. 11735003, No. 11975041, and No. 11961141004, and the Fundamental Research Funds for the Central Universities.

## APPENDIX A: COUPLINGS FROM THE COMPOSITENESS CONDITIONS

For $P_{cs}$, the ratio of the binding energy over the reduced mass is approximately $B_{P_{cs}}/\mu_{\bar{D}^*\Xi_c} \sim 1.7\%$, which, though larger than that for the deuteron with $B_D/\mu_{2m_N} \sim 0.4\%$, is still a small number. In Refs. [81,82], it was shown that the compositeness condition works for the $D_{s0}^*(2317)$ state, whose binding energy is 45 MeV as a $DK$ bound state. We thus believe that the compositeness condition is applicable in the present work.

With the assumption that the $P_{cs}$ state observed by the LHCb Collaboration can be interpreted as a molecular state of $\bar{D}^*\Xi_c$ with $J^P = 1/2^-$ or $J^P = 3/2^-$, we can calculate the couplings between the $P_{cs}$ state and its components with the compositeness condition, which is quite similar to what was done in Refs. [32,82].

According to the compositeness rule [73–75], the coupling constant $g_{P_{cs1/2}\Xi_c\bar{D}^*}$ can be determined from the fact that the renormalization constant of the wave function of a composite particle should be zero. That is,

$$Z_{P_{cs}} = 1 - \left.\frac{d\Sigma_{P_{cs}}(k_0)}{d\not{k}_0}\right|_{\not{k}_0 = m_{P_{cs}}} = 0, \tag{A1}$$

where $\Sigma_{P_{cs}}$ denotes the self-energy of $P_{cs1}$ and $P_{cs2}$. Applying the effective Lagrangians listed in Eq. (4), the self-energy $\Sigma_{P_{cs1/2}}$ reads (see Fig. 7)

$$\Sigma_{P_{cs1}}(k_0) = g^2_{P_{cs1}\Xi_c\bar{D}^*}\int\frac{d^4k_1}{i(2\pi)^4}\Phi^2[-(k_1-k_0\omega_{\Xi_c})^2]\mathcal{A}^\mu_{P_{cs1}}\frac{1}{\not{k}_1-m_{\Xi_c}}\mathcal{A}^\nu_{P_{cs1}}\frac{-g^{\mu\nu}+\frac{k_2^\mu k_2^\nu}{m^2_{D^*}}}{k_2^2-m^2_{D^*}},$$
$$\Sigma^{\mu\nu}_{P_{cs2}}(k_0) = g^2_{P_{cs2}\Xi_c\bar{D}^*}\int\frac{d^4k_1}{i(2\pi)^4}\Phi^2[-(k_1-k_0\omega_{\Xi_c})^2]\frac{1}{\not{k}_1-m_{\Xi_c}}\frac{-g^{\mu\nu}+\frac{k_2^\mu k_2^\nu}{m^2_{D^*}}}{k_2^2-m^2_{D^*}}, \tag{A2}$$

with

$$\omega_{\Xi_c} = \frac{m_{\Xi_c}}{m_{\Xi_c}+m_{D^*}},$$
$$\mathcal{A}^\mu_{P_{cs1}} = \gamma_5\left(g^{\mu\nu}-\frac{k_0^\mu k_0^\nu}{m^2_{P_{cs}}}\right)\gamma_\nu. \tag{A3}$$

The $\Phi[-p^2]=\exp(p^2/\Lambda^2)$ is the Fourier transformation of the correlation in the Gaussian form with $\Lambda$ being the size parameter which characterizes the distribution of components inside the molecule. With all the formula above and taking $\Lambda = 1.0$ GeV, we obtain the couplings between the $P_{cs}$ states and $\bar{D}^*\Xi_c$, which are $g_{P_{cs1}\Xi_c\bar{D}^*}=1.59$ for $J^P = 1/2^-$ and $g_{P_{cs2}\Xi_c\bar{D}^*}=2.76$ for $J^P=3/2^-$.

## APPENDIX B: DETERMINATION OF THE BRANCHING RATIO $\mathrm{Br}[\Xi_b\to J/\psi\Lambda\bar{K}]$

Experimentally, the branching ratio of $\Xi_b\to J/\psi\Lambda\bar{K}$ has been measured to be [83]

$$\frac{f_{\Xi_b}}{f_{\Lambda_b}}\times\frac{\mathrm{Br}[\Xi_b\to J/\psi\Lambda\bar{K}]}{\mathrm{Br}[\Lambda_b\to J/\psi\Lambda]} = (4.19\pm0.29\pm0.15)\times10^{-2}, \tag{B1}$$

where $f_{\Xi_b}$ and $f_{\Lambda_b}$ refer to the $b$ quark fragmentation fractions into $\Xi_b^-$ and $\Lambda_b^0$, the ratio of which is [84]

$$\frac{f_{\Xi_b}}{f_{\Lambda_b}} = (6.7\pm0.5\pm0.5\pm2.0)\times10^{-2}, \tag{B2}$$

while the branching ratio of $\Lambda_b\to J/\psi\Lambda$ has been measured by the CDF Collaboration [85]

$$\mathrm{Br}[\Lambda_b\to J/\psi\Lambda] = (3.7\pm1.7\pm0.7)\times10^{-4}. \tag{B3}$$

With all the ratios given above, one can compute the branching ratio of $\Xi_b\to J/\psi\Lambda\bar{K}$

$$\mathrm{Br}[\Xi_b\to J/\psi\Lambda\bar{K}] = (2.31\pm1.37)\times10^{-4}. \tag{B4}$$

The large uncertainty can be traced back to the experimental uncertainty in the branching ratio $\mathrm{Br}[\Lambda_b\to J/\psi\Lambda]$, which accounts for about 50%, and the large uncertainty in the ratio of fragmentation fractions coming from the estimation of SU(3) breaking effects [84].

## APPENDIX C: COUPLINGS FROM THE UNITARY APPROACH

In our convention, the $J/\psi\Lambda$ partial decay widths of the $P_{cs}$ state with $J^P=1/2^-$ and $3/2^-$ are expressed as

$$\Gamma_{P_{cs1}\to J/\psi\Lambda} = \frac{1}{2}\frac{g^2_{P_{cs1}J/\psi\Lambda}}{8\pi}\frac{1}{m^2_{P_{cs}}}|q|\sum|\mathcal{A}_{P_{cs1}}|^2,$$
$$\Gamma_{P_{cs2}\to J/\psi\Lambda} = \frac{1}{4}\frac{g^2_{P_{cs2}J/\psi\Lambda}}{8\pi}\frac{1}{m^2_{P_{cs}}}|q|\sum|\mathcal{A}_{P_{cs2}}|^2, \tag{C1}$$

where the modules of amplitude squared are

$$\sum|\mathcal{A}_{P_{cs1}}|^2 = \frac{((m_\Lambda+m_{P_{cs}})^2-m^2_{J/\psi})((m^2_{J/\psi}-m^2_\Lambda)^2+2m^2_{P_{cs}}(5m^2_{J/\psi}-m^2_\Lambda)+m^4_{P_{cs}})}{2m^2_{J/\psi}m^2_{P_{cs}}},$$
$$\sum|\mathcal{A}_{P_{cs2}}|^2 = \frac{((m_\Lambda+m_{P_{cs}})^2-m^2_{J/\psi})((m^2_{J/\psi}-m^2_\Lambda)^2+2m^2_{P_{cs}}(5m^2_{J/\psi}-m^2_\Lambda)+m^4_{P_{cs}})}{3m^2_{J/\psi}m^2_{P_{cs}}}, \tag{C2}$$

in which $q$ denotes the momentum of $J/\psi$ in the rest frame of the $P_{cs}$ state. With the expressions above, one can match the couplings obtained in Ref. [47] to those in Eq. (4), the values of which are $g_{P_{cs1}J/\psi\Lambda}=0.07$, $g_{P_{cs2}J/\psi\Lambda}=0.27$, $g_{P_{cs1}\Xi_c\bar{D}^*}=1.25$, and $g_{P_{cs2}\Xi_c\bar{D}^*}=2.17$.

[1] R. Aaij *et al.* (LHCb Collaboration), Phys. Rev. Lett. **115**, 072001 (2015).
[2] J.-J. Wu, R. Molina, E. Oset, and B. S. Zou, Phys. Rev. Lett. **105**, 232001 (2010).
[3] J.-J. Wu, R. Molina, E. Oset, and B. S. Zou, Phys. Rev. C **84**, 015202 (2011).
[4] W. L. Wang, F. Huang, Z. Y. Zhang, and B. S. Zou, Phys. Rev. C **84**, 015203 (2011).
[5] Z.-C. Yang, Z.-F. Sun, J. He, X. Liu, and S.-L. Zhu, Chin. Phys. C **36**, 6 (2012).
[6] S. G. Yuan, K. W. Wei, J. He, H. S. Xu, and B. S. Zou, Eur. Phys. J. A **48**, 61 (2012).
[7] J.-J. Wu, T. S. H. Lee, and B. S. Zou, Phys. Rev. C **85**, 044002 (2012).
[8] C. Garcia-Recio, J. Nieves, O. Romanets, L. L. Salcedo, and L. Tolos, Phys. Rev. D **87**, 074034 (2013).
[9] C. W. Xiao, J. Nieves, and E. Oset, Phys. Rev. D **88**, 056012 (2013).
[10] T. Uchino, W.-H. Liang, and E. Oset, Eur. Phys. J. A **52**, 43 (2016).
[11] M. Karliner and J. L. Rosner, Phys. Rev. Lett. **115**, 122001 (2015).
[12] L. Roca, J. Nieves, and E. Oset, Phys. Rev. D **92**, 094003 (2015).
[13] J. He, Phys. Lett. B **753**, 547 (2016).
[14] C. W. Xiao and U. G. Meißner, Phys. Rev. D **92**, 114002 (2015).
[15] R. Chen, X. Liu, X.-Q. Li, and S.-L. Zhu, Phys. Rev. Lett. **115**, 132002 (2015).
[16] H.-X. Chen, W. Chen, X. Liu, T. G. Steele, and S.-L. Zhu, Phys. Rev. Lett. **115**, 172001 (2015).
[17] T. J. Burns, Eur. Phys. J. A **51**, 152 (2015).
[18] C.-W. Shen, F.-K. Guo, J.-J. Xie, and B.-S. Zou, Nucl. Phys. **A954**, 393 (2016).
[19] L. Geng, J. Lu, and M. P. Valderrama, Phys. Rev. D **97**, 094036 (2018).
[20] M.-Z. Liu, F.-Z. Peng, M. Sánchez Sánchez, and M. P. Valderrama, Phys. Rev. D **98**, 114030 (2018).
[21] L. Maiani, A. D. Polosa, and V. Riquer, Phys. Lett. B **749**, 289 (2015).
[22] R. F. Lebed, Phys. Lett. B **749**, 454 (2015).
[23] Z.-G. Wang, Eur. Phys. J. C **76**, 70 (2016).
[24] F.-K. Guo, U.-G. Meißner, W. Wang, and Z. Yang, Phys. Rev. D **92**, 071502 (2015).
[25] X.-H. Liu, Q. Wang, and Q. Zhao, Phys. Lett. B **757**, 231 (2016).
[26] R. Aaij *et al.* (LHCb Collaboration), Phys. Rev. Lett. **122**, 222001 (2019).
[27] H.-X. Chen, W. Chen, and S.-L. Zhu, Phys. Rev. D **100**, 051501 (2019).
[28] R. Chen, Z.-F. Sun, X. Liu, and S.-L. Zhu, Phys. Rev. D **100**, 011502 (2019).
[29] J. He, Eur. Phys. J. C **79**, 393 (2019).
[30] M.-Z. Liu, Y.-W. Pan, F.-Z. Peng, M. Sánchez Sánchez, L.-S. Geng, A. Hosaka, and M. P. Valderrama, Phys. Rev. Lett. **122**, 242001 (2019).
[31] Y. Shimizu, Y. Yamaguchi, and M. Harada, arXiv:1904.00587.
[32] C.-J. Xiao, Y. Huang, Y.-B. Dong, L.-S. Geng, and D.-Y. Chen, Phys. Rev. D **100**, 014022 (2019).
[33] Z.-H. Guo and J. A. Oller, Phys. Lett. B **793**, 144 (2019).
[34] C. Fernández-Ramírez, A. Pilloni, M. Albaladejo, A. Jackura, V. Mathieu, M. Mikhasenko, J. A. Silva-Castro, and A. P. Szczepaniak (JPAC Collaboration), Phys. Rev. Lett. **123**, 092001 (2019).
[35] C. W. Xiao, J. Nieves, and E. Oset, Phys. Rev. D **100**, 014021 (2019).
[36] Y. Yamaguchi, H. Garcia-Tecocoatzi, A. Giachino, A. Hosaka, E. Santopinto, S. Takeuchi, and M. Takizawa, Phys. Rev. D **101**, 091502 (2020).
[37] Q. Wu and D.-Y. Chen, Phys. Rev. D **100**, 114002 (2019).
[38] M. P. Valderrama, Phys. Rev. D **100**, 094028 (2019).
[39] M.-Z. Liu, T.-W. Wu, M. Sánchez Sánchez, M. P. Valderrama, L.-S. Geng, and J.-J. Xie, Phys. Rev. D **103**, 054004 (2021).
[40] Y.-H. Lin and B.-S. Zou, Phys. Rev. D **100**, 056005 (2019).
[41] A. Ali, I. Ahmed, M. J. Aslam, A. Y. Parkhomenko, and A. Rehman, J. High Energy Phys. 10 (2019) 256.
[42] Z.-G. Wang, Int. J. Mod. Phys. A **35**, 2050003 (2020).
[43] A. Ali and A. Y. Parkhomenko, Phys. Lett. B **793**, 365 (2019).
[44] S. X. Nakamura, Phys. Rev. D **103**, L111503 (2021).
[45] R. Aaij *et al.* (LHCb Collaboration), arXiv:2012.10380.
[46] F.-Z. Peng, M.-J. Yan, M. Sánchez Sánchez, and M. P. Valderrama, arXiv:2011.01915.
[47] C. W. Xiao, J. J. Wu, and B. S. Zou, Phys. Rev. D **103**, 054016 (2021).
[48] J.-T. Zhu, L.-Q. Song, and J. He, Phys. Rev. D **103**, 074007 (2021).
[49] X.-K. Dong, F.-K. Guo, and B.-S. Zou, Progr. Phys. **41**, 65 (2021).
[50] M.-Z. Liu, Y.-W. Pan, and L.-S. Geng, Phys. Rev. D **103**, 034003 (2021).
[51] R. Chen, Eur. Phys. J. C **81**, 122 (2021).
[52] C. W. Xiao, J. Nieves, and E. Oset, Phys. Lett. B **799**, 135051 (2019).
[53] B. Wang, L. Meng, and S.-L. Zhu, Phys. Rev. D **101**, 034018 (2020).
[54] T. J. Burns and E. S. Swanson, Phys. Rev. D **100**, 114033 (2019).
[55] F.-Z. Peng, J.-X. Lu, M. Sánchez Sánchez, M.-J. Yan, and M. P. Valderrama, Phys. Rev. D **103**, 014023 (2021).
[56] H. Xu, Q. Li, C.-H. Chang, and G.-L. Wang, Phys. Rev. D **101**, 054037 (2020).
[57] G.-J. Wang, R. Chen, L. Ma, X. Liu, and S.-L. Zhu, Phys. Rev. D **94**, 094018 (2016).
[58] U. Özdem and K. Azizi, Eur. Phys. J. C **78**, 379 (2018).
[59] E. Ortiz-Pacheco, R. Bijker, and C. Fernández-Ramírez, J. Phys. G **46**, 065104 (2019).
[60] Y.-J. Xu, Y.-L. Liu, and M.-Q. Huang, Eur. Phys. J. C **81**, 421 (2021).
[61] U. Özdem, Eur. Phys. J. C **81**, 277 (2021).
[62] U. Özdem, Chin. Phys. C **45**, 023119 (2021).
[63] X.-Z. Ling, M.-Z. Liu, J.-X. Lu, L.-S. Geng, and J.-J. Xie, Phys. Rev. D **103**, 116016 (2021).
[64] H.-X. Chen, L.-S. Geng, W.-H. Liang, E. Oset, E. Wang, and J.-J. Xie, Phys. Rev. C **93**, 065203 (2016).
[65] Q. Wu, D.-Y. Chen, and R. Ji, arXiv:2103.05257.
[66] J.-X. Lu, E. Wang, J.-J. Xie, L.-S. Geng, and E. Oset, Phys. Rev. D **93**, 094009 (2016).

[67] P. A. Zyla *et al.* (Particle Data Group), Prog. Theor. Exp. Phys. **2020**, 083C01 (2020).
[68] H.-Y. Cheng, Phys. Rev. D **56**, 2799 (1997); **99**, 079901(E) (2019).
[69] R. N. Faustov and V. O. Galkin, Phys. Rev. D **98**, 093006 (2018).
[70] H.-N. Li, C.-D. Lu, and F.-S. Yu, Phys. Rev. D **86**, 036012 (2012).
[71] T. Gutsche, M. A. Ivanov, J. G. Körner, V. E. Lyubovitskij, P. Santorelli, and N. Habyl, Phys. Rev. D **91**, 074001 (2015); **91**, 119907(E) (2015).
[72] R. S. Azevedo and M. Nielsen, Phys. Rev. C **69**, 035201 (2004).
[73] S. Weinberg, Phys. Rev. **130**, 776 (1963).
[74] A. Salam, Nuovo Cimento **25**, 224 (1962).
[75] K. Hayashi, M. Hirayama, T. Muta, N. Seto, and T. Shirafuji, Fortschr. Phys. **15**, 625 (1967).
[76] N. A. Tornqvist, Nuovo Cimento Soc. Ital. Fis. A **107**, 2471 (1994).
[77] N. A. Tornqvist, Z. Phys. C **61**, 525 (1994).
[78] M. P. Locher, Y. Lu, and B. S. Zou, Z. Phys. A **347**, 281 (1994).
[79] X.-Q. Li, D. V. Bugg, and B.-S. Zou, Phys. Rev. D **55**, 1421 (1997).
[80] K. Azizi, Y. Sarac, and H. Sundu, Phys. Rev. D **103**, 094033 (2021).
[81] A. Faessler, T. Gutsche, V. E. Lyubovitskij, and Y.-L. Ma, Phys. Rev. D **76**, 014005 (2007).
[82] C.-J. Xiao, D.-Y. Chen, and Y.-L. Ma, Phys. Rev. D **93**, 094011 (2016).
[83] R. Aaij *et al.* (LHCb Collaboration), Phys. Lett. B **772**, 265 (2017).
[84] R. Aaij *et al.* (LHCb Collaboration), Phys. Rev. D **99**, 052006 (2019).
[85] F. Abe *et al.* (CDF Collaboration), Phys. Rev. D **55**, 1142 (1997).